

Benzylic C(sp³)—H Bond Oxidation with Ketone Selectivity by a Cobalt(IV)-Oxo Embedded in a β -Barrel Protein

Dong Wang,^[a] Aaron A. Ingram,^[a] Akira Okumura,^[a] Thomas P. Spaniol,^[a]
Ulrich Schwaneberg,^[b] and Jun Okuda^{*[a]}

Artificial metalloenzymes have emerged as biohybrid catalysts that allow to combine the reactivity of a metal catalyst with the flexibility of protein scaffolds. This work reports the artificial metalloenzymes based on the β -barrel protein nitrobindin NB4, in which a cofactor [Co^{II}X(Me₃TACD-Mal)]⁺X[−] (X = Cl, Br; Me₃TACD = *N,N,N'*-trimethyl-1,4,7,10-tetraazacyclododecane, Mal = CH₂CH₂CH₂NC₄H₂O₂) was covalently anchored via a Michael addition reaction. These biohybrid catalysts showed higher efficiency than the free cobalt complexes for the

oxidation of benzylic C(sp³)—H bonds in aqueous media. Using commercially available oxone (2KHSO₅·KHSO₄·K₂SO₄) as oxidant, a total turnover number of up to 220 and 97% ketone selectivity were achieved for tetralin. As catalytically active intermediate, a mononuclear terminal cobalt(IV)-oxo species [Co(IV)=O]²⁺ was generated by reacting the cobalt(II) cofactor with oxone in aqueous solution and characterized by ESI-TOF MS.

Introduction

Selective functionalization of specific C—H bonds remains challenging due to their high bond dissociation energy.^[1–4] In recent years, there has been growing interest in the development of artificial metalloenzymes as catalysts for C—H bond functionalization.^[5–8] In particular, mimics of cytochrome P450 enzymes with iron porphyrins are well-known to activate C—H bonds.^[9–14]

Until recently, cobalt complexes have barely been known to catalyze C—H bond oxidation with high activity.^[15–23] The mechanism of C—H bond oxidation using cobalt catalysts has been shown to involve the formation of a high-valent cobalt(IV)-oxo intermediate, which can abstract a hydrogen atom from the substrate to form a carbon-centered radical that converts alkanes to alcohols and ketones.^[16,24–26]

Homogeneous biohybrid catalysts, so-called artificial metalloenzymes (ArMs), contain a synthetic metal cofactor attached to the protein scaffold by supramolecular, dative, covalent binding or metal substitutions.^[27–30] Versatile protein scaffolds, such as myoglobin,^[31] streptavidin,^[32] nitrobindin,^[33–37]

hemoprotein,^[38,39] HaloTag,^[40] are available for the construction of artificial metalloenzymes. The secondary coordination sphere provided by the amino acid residues of the protein stabilizes both the cofactor and intermediates and alter its reactivity and selectivity in chemical reactions.^[30,41] In the context of C—H bond oxidation, incorporation of a [Fe^{III}(TAML)][−] cofactor (TAML = Tetra Amido Macrocyclic Ligand) into streptavidin allowed to enable the enantioselective hydroxylation of benzylic C(sp³)—H bonds.^[42] An artificial metalloenzyme based on myoglobin reconstituted with a manganese porphycene cofactor was shown to catalyze the oxidation of ethylbenzene using H₂O₂ as the terminal oxidant.^[43]

In this study, we synthesized cobalt complexes with a maleimide linker [Co^{II}X(Me₃TACD-Mal)]⁺X[−] (X = Cl, Br; Me₃TACD = *N,N,N'*-trimethyl-1,4,7,10-tetraazacyclododecane, Mal = CH₂CH₂CH₂NC₄H₂O₂) and conjugated them with a β -barrel protein NB4 to form artificial metalloenzymes for the oxidation of C—H bonds. We assume that the secondary coordination sphere provided by NB4 affects the catalytic activity of the cobalt cofactor.

Results and Discussion

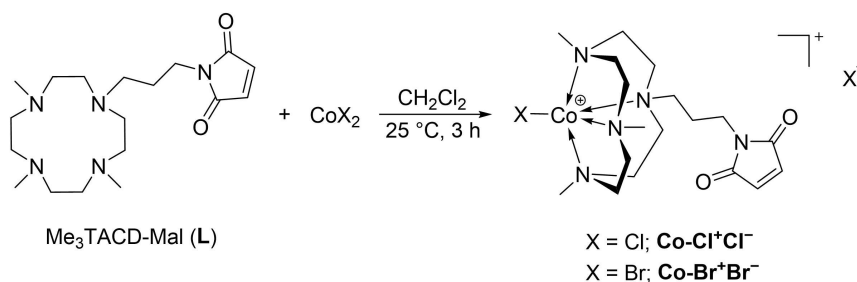
Cobalt(II) catalyst precursors Co—X⁺X[−] (X = Cl, Br) containing the macrocyclic ligand Me₃TACD-Mal (L) were straightforwardly prepared, isolated as violet (Co—Cl⁺Cl[−]) or blue crystals (Co—Br⁺Br[−]) (Scheme 1), and characterized by single crystal X-ray crystallography (Figure 1 and Supporting Information). Selected bond distances and angles are listed in Tables S3 and S5 in the Supporting Information. Both complexes have a five-coordinate, square pyramidal cobalt(II) center (τ_5 = 0.0008 for Co—Cl⁺Cl[−] and 0.0068 for Co—Br⁺Br[−]) with four nitrogen atoms of the macrocyclic ligand L in equatorial positions and one halogen atom in the axial position. The average Co—N_{basal} bond distance of Co—Br⁺Br[−] (2.156 Å) is comparable to that of

[a] D. Wang, A. A. Ingram, A. Okumura, Dr. T. P. Spaniol, Prof. Dr. J. Okuda
Institute of Inorganic Chemistry
RWTH Aachen University
52074 Aachen (Germany)
E-mail: jun.okuda@ac.rwth-aachen.de

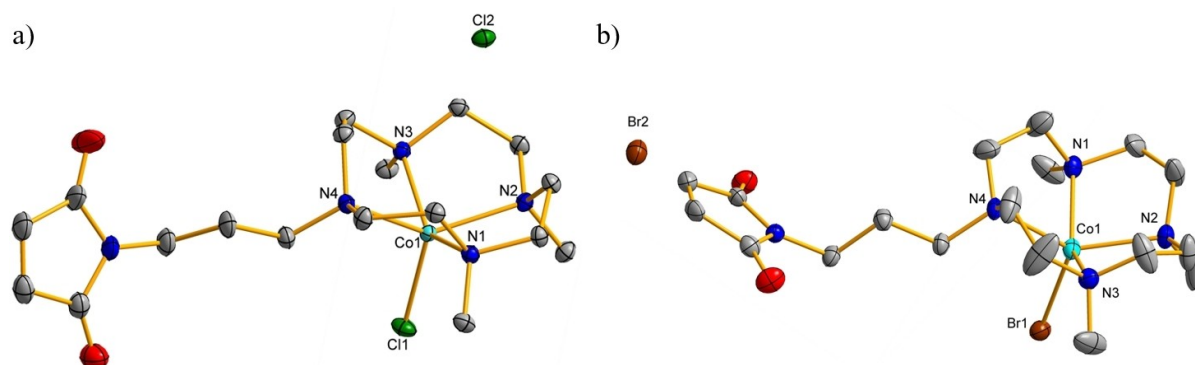
[b] Prof. Dr. U. Schwaneberg
Institute of Biotechnology
RWTH Aachen University
52074 Aachen (Germany)

Supporting information for this article is available on the WWW under <https://doi.org/10.1002/chem.202303066>

© 2023 The Authors. Chemistry - A European Journal published by Wiley-VCH GmbH. This is an open access article under the terms of the Creative Commons Attribution Non-Commercial NoDerivs License, which permits use and distribution in any medium, provided the original work is properly cited, the use is non-commercial and no modifications or adaptations are made.



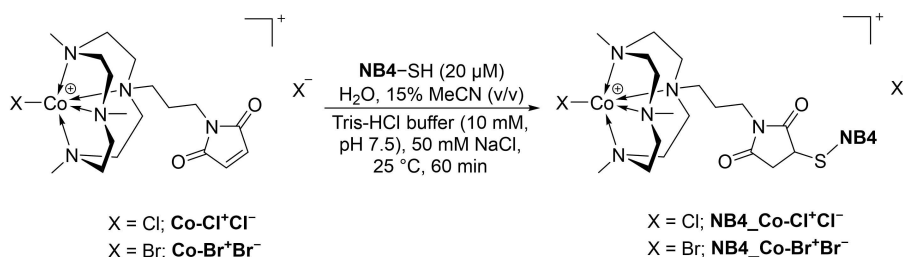
Scheme 1. Synthesis of cofactors.

Figure 1. X-ray crystal structures of (a) **Co-Cl⁺Cl⁻** and (b) **Co-Br⁺Br⁻** with displacement parameters drawn at the 50% probability level. Hydrogen atoms and solvent molecules are omitted for clarity.

Co-Cl⁺Cl⁻ (2.158 Å) and with other bond distances reported for cobalt complexes with the parent TACD ligand.^[44–46] As expected, the Co–Hal_{axial} bond distance of **Co-Cl⁺Cl⁻** (2.2566(8) Å) is shorter than that of **Co-Br⁺Br⁻** (2.3766(7) Å). The N–Co–N bond angles between two neighboring nitrogen atoms around the Co(II)-center are in the range of 81.16(9)°–82.75(9)° for **Co-Cl⁺Cl⁻** and **Co-Br⁺Br⁻**. The bond angles of N–Co–N with two opposite nitrogen atoms are in the range of 136.32(9)°–137.59(13)°, comparable to the reported data.^[44–46]

Cobalt(II) complexes with the maleimide linker **Co-Cl⁺Cl⁻** and **Co-Br⁺Br⁻** were covalently attached by a Michael addition reaction to the cysteine residue C96 of the engineered nitrobindin variant NB4 (M75L/H76L/Q96C/M148L/H158L; Figure S21 in Supporting Information; Scheme 2). The biohybrid catalysts were purified by centrifugation and size exclusion chromatography to remove any unreacted cobalt compounds. The conjugation efficiencies (determined by inductively coupled

plasma atomic emission spectroscopy, ICP-AES, Table S8) of the cobalt(II) complexes in NB4 were around 90%, suggesting that one cobalt ion per NB4 protein molecule was incorporated. Since the cobalt cofactors might be non-specifically bound to NB4 through non-covalent binding or other interactions, the bioconjugation yield was further confirmed by cysteine titration using a maleimide-bearing fluorescence indicator ThioGlo-1 (Figure S20). The control measurement of the NaPB buffer (100 mM, pH 8.0) and the cobalt complexes only showed a very low fluorescence intensity. Upon addition of ThioGlo-1 to the solutions of the biohybrid catalysts, a slightly higher fluorescence intensity compared to the NaPB buffer, and the free cofactors was observed, while the sample of NB4 showed a significantly increased fluorescence after the addition of ThioGlo-1. Compared to the solution of free NB4, samples of **NB4-Co-Cl⁺Cl⁻** and **NB4-Co-Br⁺Br⁻** exhibited only 10% fluorescence, indicating a coupling efficiency of approximately



Scheme 2. Coupling of cobalt cofactors to C96 of NB4.

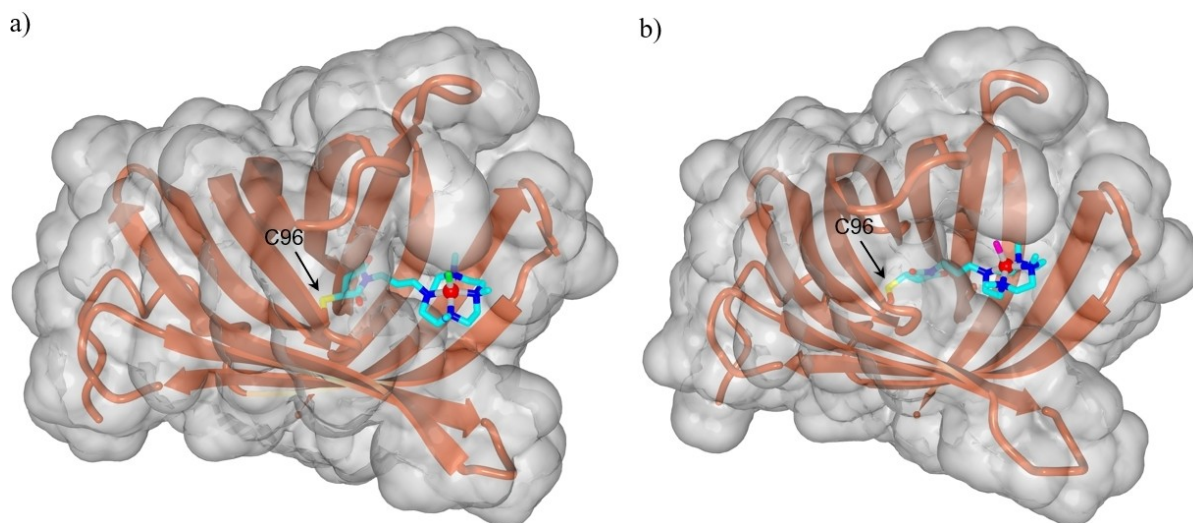


Figure 2. Representation of the cavity size in the monomeric structures of **NB4_Co-Cl⁺Cl⁻** (a) and **NB4_Co-Br⁺Br⁻** (b) calculated using the software YASARA Structure. Cobalt is represented as a red ball.

90%. The conjugation yields determined by cysteine titration are similar to those obtained from ICP-AES, suggesting that the cobalt cofactors are covalently bound to NB4.

The protein structures calculated by YASARA software (Figure 2) indicated that the cavity of NB4 (volume 855 Å³) is sufficiently large to accommodate the cobalt cofactors (van der Waals volumes: **Co-Cl⁺Cl⁻**, 417 Å³; **Co-Br⁺Br⁻**, 419 Å³). Electro-spray ionization time-of-flight mass spectrometry (ESI-TOF MS) analysis indicated the attachment of the cobalt catalyst to the protein by covalent binding (Figures S17–S19 and Table S7 in the Supporting Information). The calculated mass for catalysts **NB4_Co-Cl⁺Cl⁻** ($m/z=19,898$) and **NB4_Co-Br⁺Br⁻** ($m/z=19,987$), in which one cofactor molecule is bound to the protein scaffold, was observed in the ESI-TOF MS spectra.

The secondary structure of the biohybrid catalysts was investigated by circular dichroism (CD) spectroscopy at 25 °C in Tris-HCl buffer (10 mM, pH 7.5; 50 mM NaCl) with 15% MeCN. Both biohybrid catalysts showed a characteristic minimum at $\lambda=215$ nm, which is similar to that of NB4 (Figures S12 and S13 in the Supporting Information). The thermal stability of **NB4_Co-Br⁺Br⁻** was investigated between 25 and 60 °C in sodium phosphate buffer (100 mM, pH 8.0) with 15% MeCN used for the catalysis. The β -barrel structure of **NB4_Co-Br⁺Br⁻** was retained at temperatures of up to 40 °C (Figure 3).

The catalytic activity was initially performed for the oxidation of ethylbenzene ($BDE_{C-H}=87$ kcal/mol)^[47,48] using 2 equivalents of commercially available oxone ($2KHSO_5 \cdot KHSO_4 \cdot K_2SO_4$) in sodium phosphate buffer with 15% MeCN as co-solvent under argon atmosphere. Under these conditions, 1-phenylethanol and acetophenone were formed in the presence of the cobalt cofactors **Co-Cl⁺Cl⁻** or **Co-Br⁺Br⁻** and the corresponding biohybrid catalysts **NB4_Co-Cl⁺Cl⁻** or **NB4_Co-Br⁺Br⁻**. No other over-oxidized products were observed (Table 1). The total turnover number (TTON) and the ketone selectivity of catalytic reactions with both biohybrid catalysts were higher than those obtained with the protein-free

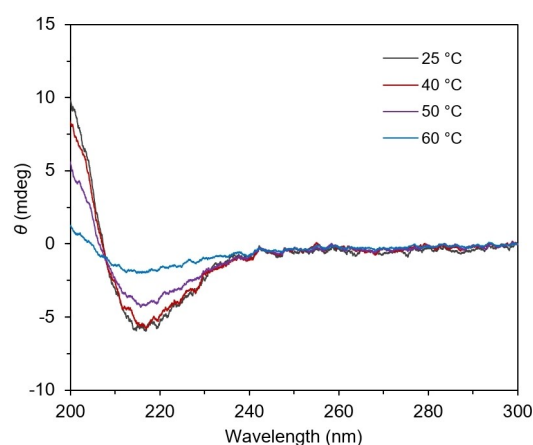
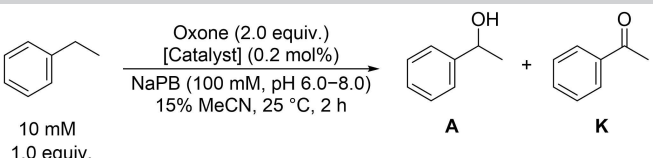


Figure 3. CD spectra of **NB4_Co-Br⁺Br⁻** in sodium phosphate buffer (100 mM, pH 8.0) with 15% MeCN at 25 °C (black), 40 °C (red), 50 °C (purple) and 60 °C (blue).

catalysts under similar reaction conditions. We hypothesize that NB4 provides an environment for the cobalt cofactor during the catalysis, which prevents them from degrading or from being consumed by other side reactions such as ligand exchange and decomposition in the buffer solution. Moreover, the hydrophobic cavity of NB4 allows nonpolar ethylbenzene molecules to diffuse faster, increasing the local concentration of ethylbenzene near the catalyst. Both biohybrid catalysts showed higher catalytic activity and ketone selectivity under basic conditions (pH 8.0) than under acidic conditions (pH 6.0). The reaction using **NB4_Co-Br⁺Br⁻** as catalyst led to a TTON of 89 with a pronounced ketone selectivity of 96% (Table 1, entry 8), while **NB4_Co-Cl⁺Cl⁻** catalyzed the oxidation of ethylbenzene with a lower TTON of 70 (Table 1, entry 6). The catalytic reactions with other co-solvents such as acetone, THF and 1,4-dioxane showed lower TTON compared to using MeCN as co-solvent. Furthermore, the presence of Tris-HCl buffer at pH 8.0 appears to negatively affect the activity of the catalyst **NB4_**

Table 1. Catalytic oxidation of ethylbenzene with oxone.

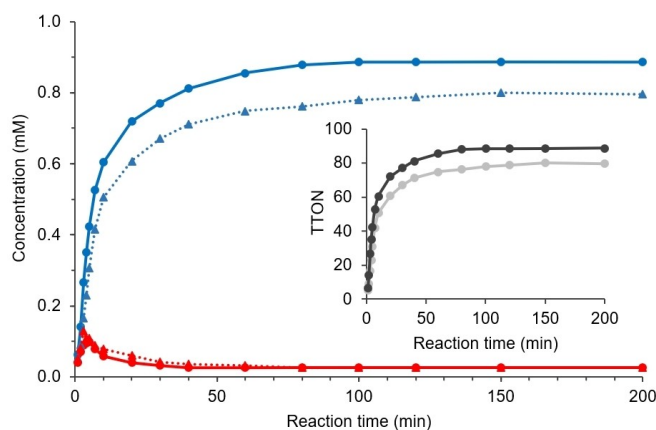
<div style="text-align: center;">  </div>					
Entry	Catalyst	pH	[K]/[A] ^[a]	TTON ^[b]	Ketone selectivity [%]
1	Co–Cl ⁺ Cl [–]	6.0	9.1	47	90
2	Co–Cl ⁺ Cl [–]	8.0	10.8	69	92
3	Co–Br ⁺ Br [–]	6.0	10.6	55	91
4	Co–Br ⁺ Br [–]	8.0	11.9	80	92
5	NB4_Co–Cl ⁺ Cl [–]	6.0	15.1	56	94
6	NB4_Co–Cl ⁺ Cl [–]	8.0	16.9	70	94
7	NB4_Co–Br ⁺ Br [–]	6.0	20.4	65	95
8	NB4_Co–Br ⁺ Br [–]	8.0	21.8	89	96
9	NB4_Co–Br ⁺ Br [–]	8.0 ^[c]	5.7	14	85
10 ^[d]	NB4_Co–Br ⁺ Br [–]	8.0	19.5	77	95
11 ^[e]	NB4_Co–Br ⁺ Br [–]	8.0	14.9	38	94
12 ^[f]	NB4_Co–Br ⁺ Br [–]	8.0	15.1	15	94
13 ^[g]	NB4_Co–Br ⁺ Br [–]	8.0	22.1	90	96
14 ^[h]	NB4_Co–Br ⁺ Br [–]	8.0	20.3	85	95
15	no catalyst	8.0	n.d.	< 1	n.d.
16 ^[i]	no catalyst	8.0	n.d.	< 5	n.d.

[a] Ketone to alcohol ratio, determined by GC-MS analysis. [b] TTON = ([alcohol] + 2x[ketone])/[catalyst]. [c] Tris-HCl buffer (50 mM, pH 8.0). [d] Catalysis with 15% acetone. [e] Catalysis with 15% THF. [f] Catalysis with 15% 1,4-dioxane. [g] 16 h reaction time. [h] Reaction in air. [i] Oxidation of 1-phenylethanol. Conditions: 10 mM substrate, 20 mM oxone, 15% MeCN, 25 °C, 2 h, sodium phosphate buffer (100 mM, pH 8.0). n.d. = not detected.

Co–Br⁺Br[–] by demetallizing the complex as well as by competing with substrate binding, leading to its inactivation. Longer reaction time did not affect the TTON (Table 1, entry 13), indicating that the catalytic oxidation was complete within 2 h. To investigate the sensitivity towards oxygen, the catalytic oxidation of ethylbenzene was performed in air under similar conditions as the reaction under argon atmosphere. A slightly lower TTON was observed with the biohybrid catalyst NB4_Co–Br⁺Br[–] (Table 1, entry 14), which is probably caused by further oxidative decomposition reactions of the intermediate species formed in the catalytic cycle mediated by oxone.

With a catalyst loading of 0.2 mol% and 2.0 equivalents of oxone, ethylbenzene was converted to 1-phenylethanol and acetophenone with a TTON of 80 using Co–Br⁺Br[–] as catalyst after 150 min at 25 °C, while NB4_Co–Br⁺Br[–] accelerated the oxidation to a TTON of 89 in 80 min. Only a small amount of alcohol up to 0.13 mM was formed (Scheme 3, red curve). We assume that the hydrophobic cavity of NB4 stabilizes the catalytically active cobalt species, thereby reducing its decomposition in the aqueous medium during the reaction. In both cases, acetophenone formed very fast within the first 10 min, suggesting that 1-phenylethanol was immediately oxidized.

The oxidation of 1-phenylethanol to acetophenone under similar conditions as the oxidation of ethylbenzene showed that 1-phenylethanol was oxidized by oxone using NB4_Co–Br⁺Br[–] as catalyst significantly faster than ethylbenzene



Scheme 3. Time dependent monitoring of ethylbenzene oxidation catalyzed by NB4_Co–Br⁺Br[–] (full curves) and Co–Br⁺Br[–] (dashed curves). Red, 1-phenylethanol; blue, acetophenone. Inset: TTON for the oxidation reaction with NB4_Co–Br⁺Br[–] (black) and Co–Br⁺Br[–] (grey). Conditions: 10 mM ethylbenzene, 20 mM oxone, 20 μM catalyst, 100 mM NaPB pH 8.0, 15% MeCN, 25 °C.

with a turnover number of 140 within 40 min, while the oxidation of ethylbenzene only reached a TTON of 81 in the same reaction time (Figure S4). Blank reaction without NB4_Co–Br⁺Br[–] showed that the oxidation of ethylbenzene and 1-

phenylethanol using oxone as oxidant proceeded very slowly at room temperature (Table 1, entries 15 and 16).

To gain insight into the nature of the oxidant, we monitored the reaction of $\text{Co-Br}^+\text{Br}^-$ with 5.0 equivalents of oxone in sodium phosphate buffer (100 mM, pH 8.0) with 15 % MeCN at 25 °C by UV-Vis spectroscopy (Figure 4a). Two absorption bands of cobalt cofactor were observed at $\lambda=502$ and 608 nm, which resemble the spectra for the cobalt complexes with the TACD ligands.^[16,49] The addition of oxone (5.0 equiv.) to a solution of $\text{Co-Br}^+\text{Br}^-$ (2 mM) in sodium phosphate buffer (100 mM, pH 8.0) with 15 % MeCN at 0 °C immediately generated a transient brown species, which converted to a dark green intermediate with a UV-Vis absorption band at $\lambda=542$ nm and a shoulder at $\lambda=386$ nm within a few seconds (Figure 4a, red curve). We suggest that this dark green species is the corresponding Co(IV)=O species $[\text{Co}^{\text{IV}}(\text{=O})(\text{Me}_3\text{TACD-Mal})]^{2+}$. Observation of similar Co(IV)=O species was reported in the literature when an oxidant was added to solutions containing a cobalt(II) complex.^[16,49–52] The transient brown color may indicate the coordination of oxone to the Co(II) center of $\text{Co-Br}^+\text{Br}^-$, which is rapidly converted to the Co(IV)=O species. The Co(IV)=O species formed is metastable and decomposed within a few seconds.^[53]

The metastable intermediate $[\text{Co}^{\text{IV}}(\text{=O})(\text{Me}_3\text{TACD-Mal})]^{2+}$ with a terminal Co(IV)=O bond was characterized by ESI-TOF MS. The spectrum exhibits a significant peak at $m/z=505.108$ (Figure 4b), which is in accordance with the mass and isotope distribution patterns of $[\text{Co}^{\text{IV}}(\text{=O})\text{Br}(\text{Me}_3\text{TACD-Mal})]^+$ (calcd. $m/z=505.109$).

The substrate scope (Table 2) for $\text{NB4_Co-Br}^+\text{Br}^-$ was expanded to molecules containing $\text{C}(\text{sp}^3)\text{-H}$ bonds such as benzylic alkanes and cyclohexane ($\text{BDE}_{\text{C-H}}=99 \text{ kcal mol}^{-1}$).^[54] Compared to the oxidation of ethylbenzene (Table 2, entry 1), *n*-propyl- and *n*-butylbenzene were oxidized with lower TTONs and ketone selectivity. The ethylbenzene derivatives with electron-rich substituents at *para*-position afforded higher TTONs.

Notably, tetralin and indane ($\text{BDE}_{\text{C-H}}=85.7$ and 87 kcal mol^{-1})^[55] were oxidized with high TTONs (TTON=220 and 162, respectively) and ketone selectivity (97% and 95%, respec-

tively). The catalytic activity of $\text{NB4_Co-Br}^+\text{Br}^-$ was sufficiently high for the oxidation of cyclohexane with a TTON of 29 (Table 2, entry 9). Over-oxidized products of ketones were not observed in any of these reactions.

We propose the following catalytic cycle for the oxidation of ethylbenzene using $\text{NB4_Co-Cl}^+\text{Cl}^-$ and $\text{NB4_Co-Br}^+\text{Br}^-$ (Scheme 4) based on the results of UV-Vis spectroscopy and reactivity studies. Starting from $\text{NB4_Co-X}^+\text{X}^-$, one KHSO_5 unit from oxone is coordinated to the Co(II) center by ligand substitution. The weaker acidity of HSO_5^- ($\text{p}K_a=9.4$)^[56] compared to that of HX ($\text{p}K_a=-7$ for X=Cl and $\text{p}K_a=-9$ for X=Br) should facilitate the substitution of X^- against chelating HSO_5^- . A high-valent cobalt(IV)-oxo species is presumed to form via heterolytic cleavage of the O–O bond of the coordinated KHSO_5 under expulsion of a KHSO_4 unit. The Co(IV)=O intermediate formed acts as the oxygen source, which oxidizes the benzylic $\text{C}(\text{sp}^3)\text{-H}$ bond of ethylbenzene as well as the alcohol to yield 1-phenylethanol and acetophenone as products, respectively.

Conclusions

Cobalt(II) complexes containing an NNNN-type macrocyclic ligand with a maleimide linker $\text{Me}_3\text{TACD-Mal}$ were prepared, characterized and covalently anchored in the engineered β -barrel protein NB4 to form biohybrid catalysts. The catalytically active high-valent cobalt(IV)-oxo species generated from $\text{Co-Br}^+\text{Br}^-$ was characterized by UV-Vis spectroscopy and ESI-TOF MS. This cobalt(IV)-oxo intermediate oxidizes the benzylic $\text{C}(\text{sp}^3)\text{-H}$ bond as well as benzylic alcohols to form the corresponding alcohol and ketone products. The biohybrid catalysts ($\text{NB4_Co-X}^+\text{X}^-$, X=Cl, Br) outperformed protein-free cobalt complexes in catalyzing the oxidation of benzylic substrates under mild conditions (pH 8.0, 25 °C) by exhibiting higher catalytic efficiency (TTON up to 220 for tetralin) and selectivity toward ketone products. This effect may be due to the presence of a hydrophobic cavity provided by the NB4 scaffold, which stabilizes the cobalt cofactors and increases the local concentration of the substrates.

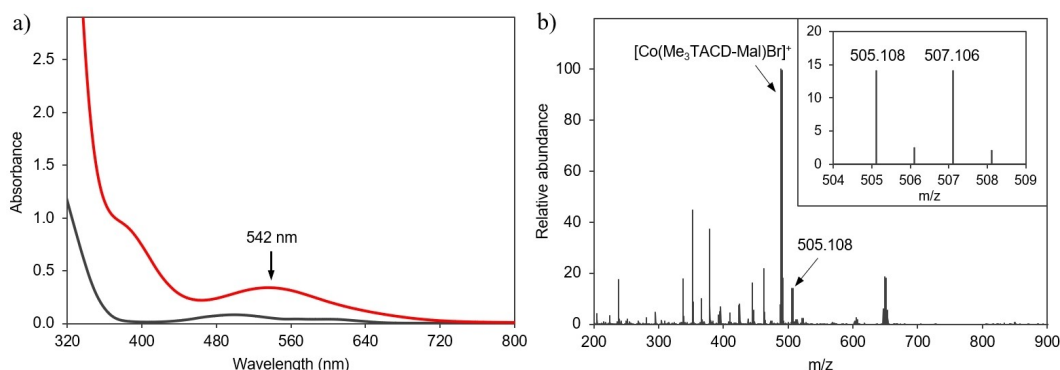
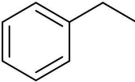
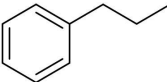
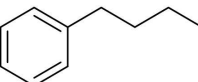
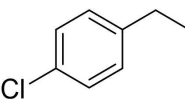
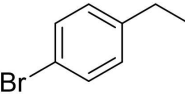
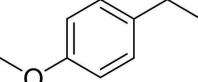
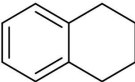
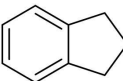
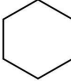


Figure 4. (a) UV-Vis spectra of $\text{Co-Br}^+\text{Br}^-$ (black curve, 2.0 mM) in sodium phosphate buffer (100 mM, pH 8.0) with 15 % MeCN. The addition of oxone (5 equiv.) leads to the immediate formation of $[\text{Co}^{\text{IV}}(\text{=O})\text{Br}(\text{Me}_3\text{TACD-Mal})]^+$ (red curve). (b) ESI-TOF MS spectrum of $[\text{Co}^{\text{IV}}(\text{=O})\text{Br}(\text{Me}_3\text{TACD-Mal})]^+$ (calculated $m/z=505.109$). The inset shows the isotope distribution patterns for $[\text{Co}^{\text{IV}}(\text{=O})\text{Br}(\text{Me}_3\text{TACD-Mal})]^+$ at $m/z=505.108$. The peaks at around $m/z=650$ are due to an impurity.

Table 2. Screening of substrates.^[a]

Entry	Substrate	[K]/[A] ^[b]	TTON ^[c]	Ketone selectivity [%]
1		21.8	89	96
2		8.2	52	89
3		18.5	38	90
4		10.1	42	91
5		9.8	62	91
6		11.6	145	92
7		36.2	220	97
8		19.8	162	95
9 ^[d]		3.1	29	76

[a] Conditions: 20 μM $\text{NB4_Co-Br}^+\text{Br}^-$, 10 mM substrate, 20 mM oxone, sodium phosphate buffer (100 mM, pH 8.0), 15% MeCN, 2 h at 25 °C. [b] Ketone to alcohol ratio, determined by GC-MS analysis. [c] $\text{TTON} = ([\text{alcohol}] + 2 \times [\text{ketone}]) / [\text{catalyst}]$. More details in Figure S5. [d] Catalysis in the presence of 15% acetone.

Experimental Section

Full details of all experiments and characterization data of the described compounds are given in the Supporting Information.

Reagents: All chemicals were obtained from commercial suppliers (Sigma-Aldrich/Merck, Alfa Aesar, TCI), unless stated otherwise. *N*-(3-bromopropyl)phthalimide,^[57] *N*-(methoxycarbonyl)maleimide^[58] and Me_3TACDH ^[59] were synthesized according to procedures previously described.

General procedure for the catalysis with purified protein: The purified $\text{NB4_Co-Cl}^+\text{Cl}^-$ or $\text{NB4_Co-Br}^+\text{Br}^-$ in the reaction buffer (100 mM NaPB, pH 8.0, total volume 500 μL , $c(\text{ArM}) = 20 \mu\text{M}$) was incubated with substrate (10 mM) and 15% acetonitrile. The reaction was started by adding 2.0 equiv. of oxone (20 mM). The reaction mixture was stirred in a thermoshaker (900 rpm) at room temperature for the given reaction time. The reaction was quenched by adding 10 μL HCl (2 M). The reaction mixture was extracted with dichloromethane (500 μL) containing nitrobenzene (1 mM) as an internal standard. The extract was analyzed with GC-MS.

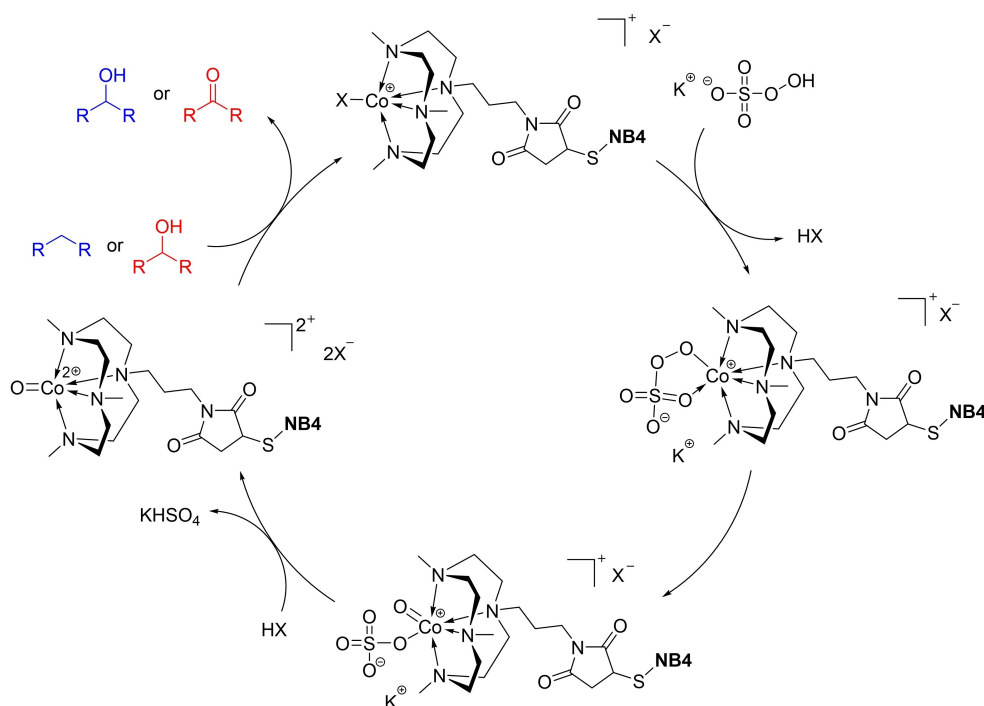
Deposition Numbers 2278290 ($\text{Me}_3\text{TACD} \cdot \text{HBr}$), 2278291 ($\text{Co-Cl}^+\text{Cl}^-$), and 2278292 ($\text{Co-Br}^+\text{Br}^-$) contain the supplementary crystallographic data for this paper. These data are provided free of charge by the joint Cambridge Crystallographic Data Centre and Fachinformationszentrum Karlsruhe Access Structures service.

Supporting Information

Experimental procedures, crystal structures, spectroscopic characterization, and additional data are available in the Supporting Information. Additional references cited within the Supporting Information.^[57–70]

Acknowledgements

We acknowledge the Bioökonomie REVER_INNO PlastiQuant (FKZ: 031B0918E) and the German Federal Ministry of Education and Research (BMBF) for financial support. We thank Dr. G. Fink



Scheme 4. Proposed reaction mechanism for the formation of Co(IV)=O species starting from NB₄-Co-X⁺X⁻ (X=Cl, Br).

for assistance with NMR experiments and Dr. D. F. Sauer for helpful discussions. Open Access funding enabled and organized by Projekt DEAL.

Conflict of Interests

The authors declare no conflict of interest.

Data Availability Statement

The data that support the findings of this study are available from the corresponding author upon reasonable request.

Keywords: artificial metalloenzyme • β -barrel protein • biohybrid catalysis • C–H bond oxidation • cobalt-oxo complex

- [1] S. Gronert, *J. Org. Chem.* **2006**, *71*, 1209–1219.
- [2] R. G. Bergman, *Nature* **2007**, *446*, 391–393.
- [3] B. Ruscic, *J. Phys. Chem. A* **2015**, *119*, 7810–7837.
- [4] J. F. Hartwig, M. A. Larsen, *ACS Cent. Sci.* **2016**, *2*, 281–292.
- [5] Y. Gu, S. N. Natoli, Z. Liu, D. S. Clark, J. F. Hartwig, *Angew. Chem. Int. Ed.* **2019**, *58*, 13954–13960.
- [6] Z. Liu, J. Huang, Y. Gu, D. S. Clark, A. Mukhopadhyay, J. D. Keasling, J. F. Hartwig, *J. Am. Chem. Soc.* **2022**, *144*, 883–890.
- [7] X. Ren, R. Fasan, *Curr. Opin. Green Sustain. Chem.* **2021**, *31*, 100494.
- [8] C. Rumo, A. Stein, J. Klehr, R. Tachibana, A. Prescimone, D. Häussinger, T. R. Ward, *J. Am. Chem. Soc.* **2022**, *144*, 11676–11684.
- [9] C. Zhang, P. Srivastava, K. Ellis-Guardiola, J. C. Lewis, *Tetrahedron* **2014**, *70*, 4245–4249.
- [10] D. M. Upp, J. C. Lewis, *Curr. Opin. Chem. Biol.* **2017**, *37*, 48–55.
- [11] C. Perez-Rizquez, A. Rodriguez-Otero, J. M. Palomo, *Org. Biomol. Chem.* **2019**, *17*, 7114–7123.

- [12] H. J. Davis, T. R. Ward, *ACS Cent. Sci.* **2019**, *5*, 1120–1136.
- [13] L. Que, Jr., W. B. Tolman, *Nature* **2008**, *455*, 333–340.
- [14] P. C. Brujininx, G. van Koten, R. J. Klein Gebbink, *Chem. Soc. Rev.* **2008**, *37*, 2716–2744.
- [15] W. Nam, I. Kim, Y. Kim, C. Kim, *Chem. Commun.* **2001**, 1262–1263.
- [16] B. Wang, Y. M. Lee, W. Y. Tcho, S. Tussupbayev, S. T. Kim, Y. Kim, M. S. Seo, K. B. Cho, Y. Dede, B. C. Keegan, T. Ogura, S. H. Kim, T. Ohta, M. H. Baik, K. Ray, J. Shearer, W. Nam, *Nat. Commun.* **2017**, *8*, 14839.
- [17] Y. Chen, H. Shi, C.-S. Lee, S.-M. Yiu, W.-L. Man, T.-C. Lau, *J. Am. Chem. Soc.* **2021**, *143*, 14445–14450.
- [18] J. Nakazawa, A. Yata, T. Hori, T. D. P. Stack, Y. Naruta, S. Hikichi, *Chem. Lett.* **2013**, *42*, 1197–1199.
- [19] G. B. Shul'pin, D. A. Loginov, L. S. Shul'pina, N. S. Ikonnikov, V. O. Idrisov, M. M. Vinogradov, S. N. Osipov, Y. V. Nelyubina, P. M. Tyubaeva, *Molecules* **2016**, *21*.
- [20] R. R. Reinig, D. Mukherjee, Z. B. Weinstein, W. Xie, T. Albright, B. Baird, T. S. Gray, A. Ellern, G. J. Miller, A. H. Winter, S. L. Bud'ko, A. D. Sadow, *Eur. J. Inorg. Chem.* **2016**, *2016*, 2486–2494.
- [21] W.-J. Hu, X.-T. Zhou, M.-Z. Sun, H.-B. Ji, *Catal. Commun.* **2021**, *159*, 106353.
- [22] R. Siedlecka, *Catalysts* **2023**, *13*.
- [23] J. B. McManus, J. D. Griffin, A. R. White, D. A. Nicewicz, *J. Am. Chem. Soc.* **2020**, *142*, 10325–10330.
- [24] D. D. Malik, Y.-M. Lee, W. Nam, *Bull. Korean Chem. Soc.* **2022**, *43*, 1075–1082.
- [25] D. Kim, J. Cho, Y.-M. Lee, R. Sarangi, W. Nam, *Chem. Eur. J.* **2013**, *19*, 14112–14118.
- [26] H.-M. Shen, L. Liu, B. Qi, M.-Y. Hu, H.-L. Ye, Y.-B. She, *J. Mol. Catal.* **2020**, *493*, 111102.
- [27] H. Yang, P. Srivastava, C. Zhang, J. C. Lewis, *ChemBioChem* **2014**, *15*, 223–227.
- [28] J. Zhao, A. Kajetanowicz, T. R. Ward, *Org. Biomol. Chem.* **2015**, *13*, 5652–5655.
- [29] D. F. Sauer, T. Himiyama, K. Tachikawa, K. Fukumoto, A. Onoda, E. Mizohata, T. Inoue, M. Bocola, U. Schwaneberg, T. Hayashi, J. Okuda, *ACS Catal.* **2015**, *5*, 7519–7522.
- [30] F. Schwizer, Y. Okamoto, T. Heinisch, Y. Gu, M. M. Pellizzoni, V. Lebrun, R. Reuter, V. Kohler, J. C. Lewis, T. R. Ward, *Chem. Rev.* **2018**, *118*, 142–231.
- [31] G. Sreenilayam, R. Fasan, *Chem. Commun.* **2015**, *51*, 1532–1534.

- [32] S. G. Keller, A. Pannwitz, H. Mallin, O. S. Wenger, T. R. Ward, *Chemistry* **2017**, *23*, 18019–18024.
- [33] A. R. Grimm, D. F. Sauer, M. D. Davari, L. Zhu, M. Bocola, S. Kato, A. Onoda, T. Hayashi, J. Okuda, U. Schwaneberg, *ACS Catal.* **2018**, *8*, 3358–3364.
- [34] D. F. Sauer, M. Wittwer, U. Markel, A. Minges, M. Spiertz, J. Schiffels, M. D. Davari, G. Groth, J. Okuda, U. Schwaneberg, *Catal. Sci. Technol.* **2021**, *11*, 4491–4499.
- [35] A. R. Grimm, D. F. Sauer, T. Polen, L. Zhu, T. Hayashi, J. Okuda, U. Schwaneberg, *ACS Catal.* **2018**, *8*, 2611–2614.
- [36] U. Markel, D. F. Sauer, J. Schiffels, J. Okuda, U. Schwaneberg, *Angew. Chem. Int. Ed.* **2019**, *58*, 4454–4464.
- [37] U. Markel, D. F. Sauer, M. Wittwer, J. Schiffels, H. Cui, M. D. Davari, K. W. Kröckert, S. Herres-Pawlis, J. Okuda, U. Schwaneberg, *ACS Catal.* **2021**, *11*, 5079–5087.
- [38] T. Hayashi, Y. Sano, A. Onoda, *Isr. J. Chem.* **2015**, *55*, 76–84.
- [39] K. Oohora, A. Onoda, T. Hayashi, *Acc. Chem. Res.* **2019**, *52*, 945–954.
- [40] S. Fischer, T. R. Ward, A. D. Liang, *ACS Catal.* **2021**, *11*, 6343–6347.
- [41] T. K. Hyster, T. R. Ward, *Angew. Chem. Int. Ed.* **2016**, *55*, 7344–7357.
- [42] J. Serrano-Plana, C. Rumo, J. G. Rebelein, R. L. Peterson, M. Barnett, T. R. Ward, *J. Am. Chem. Soc.* **2020**, *142*, 10617–10623.
- [43] K. Oohora, H. Meichin, Y. Kihira, H. Sugimoto, Y. Shiro, T. Hayashi, *J. Am. Chem. Soc.* **2017**, *139*, 18460–18463.
- [44] H. H. Cui, M. M. Ding, X. D. Zhang, W. Lv, Y. Q. Zhang, X. T. Chen, Z. Wang, Z. W. Ouyang, Z. L. Xue, *Dalton Trans.* **2020**, *49*, 14837–14846.
- [45] H. H. Cui, Y. Q. Zhang, X. T. Chen, Z. Wang, Z. L. Xue, *Dalton Trans.* **2019**, *48*, 10743–10752.
- [46] J. Cho, R. Sarangi, H. Y. Kang, J. Y. Lee, M. Kubo, T. Ogura, E. I. Solomon, W. Nam, *J. Am. Chem. Soc.* **2010**, *132*, 16977–16986.
- [47] S. Evans, J. R. Lindsay Smith, *J. Chem. Soc. Perkin Trans. 2* **2000**, 1541–1552.
- [48] L. Bering, S. Manna, A. P. Antonchick, *Chemistry* **2017**, *23*, 10936–10946.
- [49] A. Ali, W. Akram, H. Y. Liu, *Molecules* **2018**, *24*.
- [50] J. Yang, H. T. Dong, M. S. Seo, V. A. Larson, Y.-M. Lee, J. Shearer, N. Lehnert, W. Nam, *J. Am. Chem. Soc.* **2021**, *143*, 16943–16959.
- [51] Y. Zong, X. Guan, J. Xu, Y. Feng, Y. Mao, L. Xu, H. Chu, D. Wu, *Environ. Sci. Technol.* **2020**, *54*, 16231–16239.
- [52] Y. Zong, H. Zhang, X. Zhang, W. Liu, L. Xu, D. Wu, *Appl. Catal. B* **2022**, *300*, 120722.
- [53] O. V. Nesterova, M. N. Kopylovich, D. S. Nesterov, *RSC Adv.* **2016**, *6*, 93756–93767.
- [54] Z. Tian, A. Fattahi, L. Lis, S. R. Kass, *J. Am. Chem. Soc.* **2006**, *128*, 17087–17092.
- [55] P. C. St John, Y. Guan, Y. Kim, S. Kim, R. S. Paton, *Nat. Commun.* **2020**, *11*, 2328.
- [56] S. K. Rani, D. Easwaramoorthy, I. M. Bilal, M. Palanichamy, *Appl. Catal. A* **2009**, *369*, 1–7.
- [57] R. Venkatesh, S. Kasaboina, S. Janardhan, N. Jain, R. Bantu, L. Nagarapu, *Med. Chem. Res.* **2016**, *25*, 2070–2081.
- [58] M. Wang, W.-W. Bao, W.-Y. Chang, X.-M. Chen, B.-P. Lin, H. Yang, E.-Q. Chen, *Macromolecules* **2019**, *52*, 5791–5800.
- [59] D. Mukherjee, J. Okuda, *Chem. Commun.* **2018**, *54*, 2701–2714.
- [60] A. Onoda, K. Fukumoto, M. Arlt, M. Bocola, U. Schwaneberg, T. Hayashi, *Chem. Commun.* **2012**, *48*, 9756–9758.
- [61] K. Fukumoto, A. Onoda, E. Mizohata, M. Bocola, T. Inoue, U. Schwaneberg, T. Hayashi, *ChemCatChem* **2014**, *6*, 1229–1235.
- [62] E. Krieger, G. Vriend, *Bioinformatics* **2014**, *30*, 2981–2982.
- [63] Y. Duan, C. Wu, S. Chowdhury, M. C. Lee, G. Xiong, W. Zhang, R. Yang, P. Cieplak, R. Luo, T. Lee, J. Caldwell, J. Wang, P. Kollman, *J. Comput. Chem.* **2003**, *24*, 1999–2012.
- [64] J. Wang, R. M. Wolf, J. W. Caldwell, P. A. Kollman, D. A. Case, *J. Comput. Chem.* **2004**, *25*, 1157–1174.
- [65] A. Jakalian, D. B. Jack, C. I. Bayly, *J. Comput. Chem.* **2002**, *23*, 1623–1641.
- [66] M. F. Sanner, A. J. Olson, J.-C. Spehner, *Biopolymers* **1996**, *38*, 305–320.
- [67] H. M. Key, P. Dydio, D. S. Clark, J. F. Hartwig, *Nature* **2016**, *534*, 534–537.
- [68] G. M. Sheldrick, *Acta Crystallogr.* **2015**, *C71*, 3–8.
- [69] G. M. Sheldrick, *Acta Crystallogr.* **2015**, *A71*, 3–8.
- [70] O. V. Dolomanov, L. J. Bourhis, R. J. Gildea, J. A. K. Howard, H. Puschmann, *J. Appl. Crystallogr.* **2009**, *42*, 339–341.

Manuscript received: September 21, 2023
Accepted manuscript online: October 11, 2023
Version of record online: November 30, 2023